DOI: 10.61782/fa.2025.0739

FORUM ACUSTICUM
EURONOISE 2025

RELATIONSHIP AMONG NOISE, CAVITATION STRUCTURE AND EROSION RISK IN INDUSTRIAL CENTRIFUGAL PUMPS WITH A FAN-TYPE INDUCER

Shimpei Narimatsu[1*] **Haruto Utsumi**[1] **Shinichiro Ejiri**[2] **Masahiro Miyabe**[1]
[1]Osaka Institute of Technology, Osaka, Japan
[2]Nikkiso Co., Ltd. , Tokyo, Japan

ABSTRACT

There is a strong demand for pump manufacturers to prevent problems such as noise, vibration and erosion due to cavitation before delivering products to the site. This study aims to establish a practical technique for predicting the occurrence, structure, and erosion risk of cavitation by noise measurements. A centrifugal pump with a fan-type inducer was operated to measure noise both outside and inside of pipes at various suction conditions and flow rates. Visualization experiments around the inducer were also conducted to identify the cavitation structure. In addition, the paint erosion test was conducted to estimate the cavitation erosion risk at the blades of the inducer. From these experiment results, the relationship between noise, cavitation structure and erosion risk were discussed. The overall sound pressure level measured by air-borne noise measurements was found to be characterized as the increase with the enlarged peeling area obtained from the paint erosion test. Furthermore, the overall sound pressure level measured by the liquid-borne noise measurements was also confirmed to be related with the vibration due to cavitation instability phenomena.

Keywords: *Turbopump, Cavitation, Inducer, Noise*

[*]***Corresponding author***: *m1m24426@st.oit.ac.jp*

1. INTRODUCTION

Cavitation in turbopumps is a serious problem due to the vibration, noise, and damage it causes in comparison to the stability of the pump[1]. Therefore, pump manufacturers are required to identify problems caused by cavitation before delivering products to the site. Predictions have been made by experimental methods and numerical fluid analysis, but users and designers may determine the existence of cavitation from noise. Dong[2] et al. attempted to visualize the occurrence of cavitation in centrifugal pumps and to measure liquid-borne noise with the hydrophone. The results indicate the feasibility of detecting the presence of cavitation from the over-all value of the liquid-borne noise. In terms of Air-borne noise, Chudina[3] measured audible external noise for a centrifugal pump impeller. As a result, there is a large change in the 1/2BPF (Blade Passing Frequency) before and after the occurrence of cavitation, and it is thought that the change in this frequency band may be used to detect cavitation. Černetič[4] et al. made the similar measurement and confirmed that besides discrete frequencies, there are also large changes in a wide frequency range of 20 Hz to 20 kHz, indicating that it can be used for detection. In addition, Iga[5] et al. used a centrifugal pump with the visualization system to measure the unsteady flow and external noise using the microphone during cavitation instability phenomena. As a result, it was confirmed that the external noise had a predominant swirling frequency component during the occurrence of the rotating cavitation, and the possibility of inferring the occurrence of the cavitation was reported. As described above, liquid-borne and air-borne noise measurements have shown positive results in detecting the occurrence of cavitation. However, since noise measurement is greatly affected by component materials, pump geometry, and measurement environment, various research results are

needed for further practical application. Furthermore, the prediction of cavitation erosion has been studied by numerical fluid dynamics analysis[6-7], but experimental prediction is also important due to its sophistication, as it must consider the collapse and growth of individual bubbles. In this study, a fan-type inducer, with cavitation instability phenomenon[8] confirmed at low flow rates, will be experimentally investigated and analyzed to establish a practical method for noise by investigating the occurrence and development of cavitation, its morphology, and the risk of erosion. The effects of varying the blade leading edge geometry on the cavitation collapse area and the noise are investigated.

2. EXPERIMENTAL FACILITY

2.1 Test Facility

Figure 1 indicates the experimental apparatus mainly consists of suction pipes D_s (JIS (Japan Industrial Standards) 125A), discharge pipes D_d (JIS 80A), a control valve, an ultrasonic flow meter, a vacuum pump, and a tank. A pump is placed in the test section and motor is electronically controlled to maintain the rotational speed constant at any set value. The working fluid is fresh water. The pump performance is evaluated from shaft rotational speed, torque, flow rate, and the difference of static pressure between section A and B. The flow rate is adjusted to any set value with a control valve and is measured by an ultrasonic flowmeter. The pressure of the liquid level in the tank is adjusted by a vacuum pump to change the pressure of the entire piping system. The centrifugal pump used in the present study is a vertical pump that is mainly used for transporting Liquified Natural Gas. The discharge port was modified by turning sideways to apply to Osaka Institute of

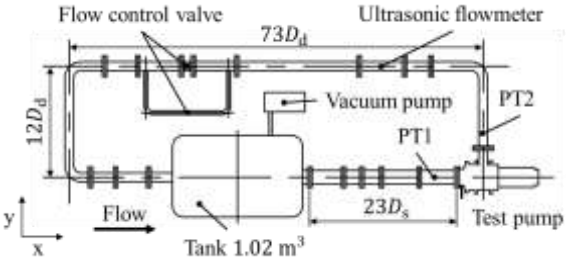

Technology test facility.

Figure 1. Test Facility

2.2 Test Pump

Figure 2 shows the cross sectional view of the test pump. The test pump has a 4-blade fan-type inducer, a 9-blade closed impeller, and an 8-vane axial diffuser with vane slit[9].

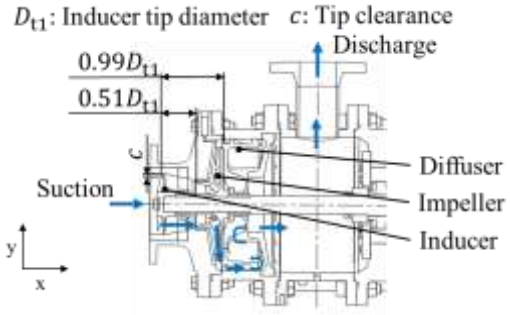

D_{t1} represents the inducer diameter. The impeller inlet is $0.51D_{t1}$ axially away from the trailing edge of the inducer and the diffuser inlet is $0.99D_{t1}$. The type number of this pump is 156 (specific speed :138 m^3/min,m,min^{-1}).

Figure 2. Cross-sectional view of the test pump

2.3 The fan-type Inducer

Figure 3 shows the external view of the fan-type inducer (Base type). Table 1 shows the primary geometrical properties of the fan-type inducer[10]. It summarizes the parameters that relate to the cavitation performance. The design parameter that represents the most significant feature of this inducer is solidity which is defined as equation (1). This type of inducer is suitable for high flow rate and low head specifications and is used in industrial applications, but few studies have been conducted. Inlet flow rate / inlet tip blade tip angle ratio, m_1 satisfies recommended value, m_1>0.4 defined as equation (2). In comparison with the design guideline of the turbopump for a rocket[11]. It indicates that flow instabilities due to backflow such as cavitation surge are unlikely to occur at the design flow rate for this inducer. In addition, inlet tip blade angle, β_{t1} meets within recommended value which should be less than 20 deg. However, the outlet tip bade angle is larger and the backflow is likely to occur at low flow rate. On the other hand, the hub / tip ratio, ν_1 is larger than the recommended value 0.25 to 0.35[11] and it suppresses to occur backflow at low flow rate because average flow velocity is relativity large at the inducer inlet. The diameter of the inducer hub is determined by that of the shaft and pump performance is well balanced by those two parameters, β_{t1} and ν_1. However, cavitation is relativity easy to occur. Furthermore, the tip

clearance ratio, c is smaller than recommended value 0.009 to 0.011 to achieve high efficiency.

Table 1. Design parameters of fan-type inducer

Number of blades [-] : n_1	4
Tip diameter [mm] : D_{t1}	125.3
Hub diameter [mm] : D_{h1}	51.0
Hub height [mm] : h_1	40.0
Solidity at tip [-] : S_t	0.77
Solidity at hub [-] : S_h	0.83
Inlet flow rate/Inlet blade tip angle ratio [-] : m_1	0.47
Inlet blade tip angle [deg.] : β_{t1}	10.5
Hub/Tip ratio [-] : ν_1	0.41
Tip clearance [mm] : c	0.65

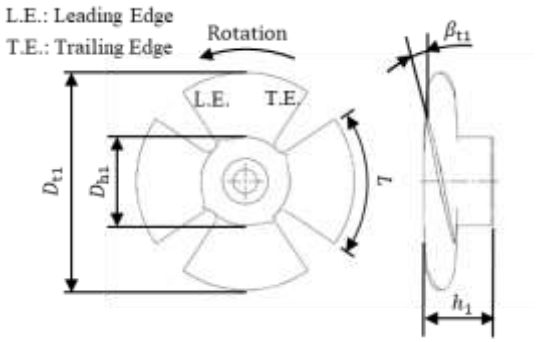

Figure 3. External view of a fan-type inducer (Base)

3. EXPERIMENTAL METHODS

3.1 NPSH test

NPSH test is conducted to measure pump cavitation performance. The pressure of the inlet is decreased by the vacuum pump, the pump total head at each cavitation number is recorded. Experiment is conducted until the condition where pump head drop is confirmed by 3 % (NPSH3). The rotational speed is 3000 min^{-1}.

3.2 Noise measurement test

Air-borne and liquid-borne noise were measured to clarify the effectiveness of noise measurements in detecting cavitation and the characteristics of the collapse sound. The locations of the air-borne and liquid-borne noise measurements are shown in Fig. 4. For the air-borne noise measurements, a microphone (BOYA, PVM1000) was placed 5 mm away from the outside wall of the casing. These measurements were based on previous studies by Saito[12]. The measured sound pressure was passed through an amplifier and frequency analyzed using an FFT (Fast Fourier Transform) analyzer(ONOSOKKI, CF-5210). The frequency range was recorded from 25 Hz to 20 kHz, which is the audible range, and from 25 Hz to 5 kHz to observe the BPF in detail. The frequency-weighted A-weighted characteristics were evaluated in consideration of human hearing. For the liquid-borne noise measurements, a hydrophone (Brüel & Kjær, Type 8103) was installed inside the pipe upstream of the inducer. The tip of the hydrophone was placed at the same position as the inner wall of the pipe. Liquid-borne sound pressure data acquired by a data logger (KEYENCE, NR-X100, CA04) was subjected to FFT analysis using a data evaluation code written in Python 3.13.2. The frequency range is 25 Hz to 5 kHz.
In this study, an anechoic chamber was not used, assuming a factory environment where industrial pumps are operated.

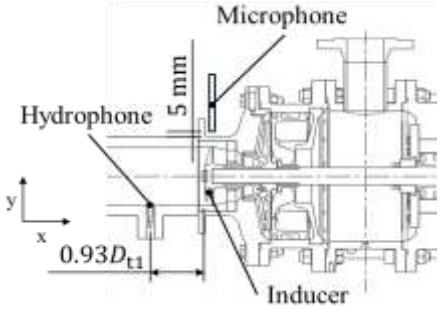

Figure 4. Positions of a microphone and a hydrophone

3.3 Visualization test

Visualization experiments were conducted to observe and identify cavitation foam. Figure 5 shows a schematic view. The inducer casing is made of acrylic, and a high-speed camera (Photron, FASTCAM Mini AX100) was used to capture images at a speed of 6,000 fps. The brightness of the images was adjusted by using a 500 W halogen light source (EARTH MAN, WLT-260).

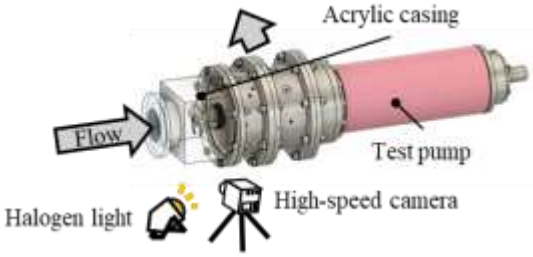

Figure 5. Schematic view of visualization test rig

3.4 Paint erosion test

Paint erosion test is conducted to observe paint removal area due to cavitation on the blade surface of a fan type inducer. Blue varnish (JIP 101) is painted on the inducer blade surface with reference to Fukaya[6]. After 30 minutes of operation with constant flow rate and cavitation number, the inducer is removed from the test stand and the condition of the blade surface is observed.

4. EXPERIMENTAL RESULTS AND DISCUSSION

4.1 Results of NPSH tests and visualization tests

Figure 6 shows the suction performance curve of the test pump and the development and form of cavitation under each operating condition. For ϕ/ϕ_d =0.50, 0.70, 1.00, and 1.20, ψ dropped sharply after maintaining a constant value with the decrease in σ. The visualization experiments revealed that cavitation occurred at the inducer (○ in the figure) and then developed into the shaft and impeller (△ and ◇ in the figure), which may be due to the blockage of the flow channel by the cavities. Focusing on ϕ/ϕ_d =0.30, vortex cavitation in reverse flow occurred in the range of σ =0.057 to 0.541 (□ in the figure). Furthermore, below σ = 0.051, a cavitation surge was observed, with intermittent cavitation expansion and contraction. Under conditions where cavitation surges occurred, the pump system vibration increased, so measurements could not be taken until the head dropped (x in the figure).

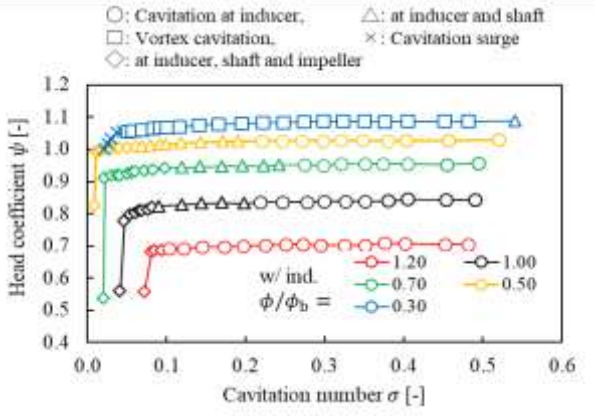

Figure 6. Suction performance curve of test pump and cavitation patterns

Next, we show the development form of cavitation based on the results of the visualization experiment. Figure 7(a) shows the cavitation morphology at the rated flow rate of the pump. σ = 0.453, cavitation occurred with the same shape on the negative pressure surface of all inducer blades. Cavitation originated at the leading edge of the blade and fluctuated at the trailing edge due to the gap leakage from the casing, confirming the release of a group of bubbles. These cavitation patterns are a mixture of sheet cavitation, crevice cavitation, and bubble cavitation[13]. Figure 7(b) shows a visualization image of the same flow rate with lower pump suction pressure. As σ decreases, the cavities expand to the trailing edges of the blades, and the leakage cavitation expands at the same time. Cavitation was also observed around the shaft and continued to the impeller inlet with a swirling element. Cavitation was also observed at the impeller inlet in Fig. 7(c), the point of 3% drop in pump head. Since the flow path between the inducer blades is not completely blocked by cavitation, the drop in pump head is considered due to channel blockage caused by cavitation in the impeller. The same cavitation development process was also observed for ϕ/ϕ_d =0.50, 0.70, and 1.20. Figure 7(d) shows the vortex cavitation in reverse flow with ϕ/ϕ_d =0.30 and σ =0.324, exhibiting a cluster of fine bubbles around the inducer blade. The cavitation form was not changed with a decline in suction pressure, and intermittent expansion and contraction of a cluster of fine bubbles were observed during the cavitation surge. Visualization experiments confirmed the cavitation occurred at the leading edge of the blades and developed in the direction of the trailing edge.

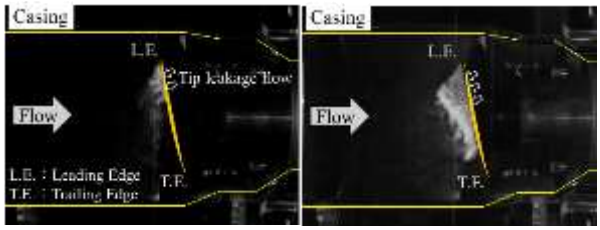

(a) ϕ/ϕ_d =1.00, σ =0.453, (b) ϕ/ϕ_d =1.00, σ =0.170

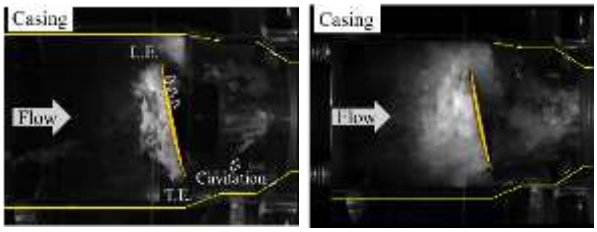

(a) ϕ/ϕ_d =1.00, σ = 0.453, (b) ϕ/ϕ_d =1.00, σ =0.170

Figure 7. Cavitation development around inducer

The following sections compare the paint removal on the suction side of the inducer blade in the paint erosion test. As shown in Fig. 8(a), a small detachment was observed from the center of the blade edge to the trailing edge at ϕ/ϕ_d =1.00 and σ =0.197. Decreasing the pump suction pressure, σ =0.052 in Fig. 8(b), shows the change to a plane delamination extending to the trailing edge of the airfoil. Figure 8(c) and (d) with ϕ/ϕ_d =1.20 also resulted in a plane delamination. For other ϕ/ϕ_d conditions, sparse and areal detachment was not observed at the point of head reduction. Cavitation collapse was stronger on the trailing edge of the inducer blade, suggesting a high risk of erosion near the trailing edge for ϕ/ϕ_d =1.00 and 1.20.

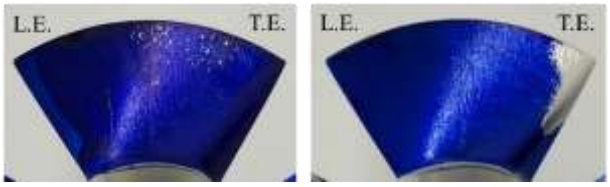

(a) ϕ/ϕ_d =1.00, σ =0.197 (b) ϕ/ϕ_d =1.00, σ =0.052

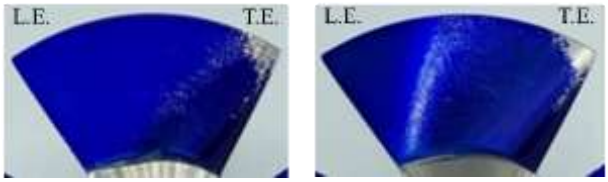

(c) ϕ/ϕ_d =1.20, σ =0.094 (b) ϕ/ϕ_d =1.20, σ =0.058

Figure 8. Paint peeling area at suction surface

4.2 Relationship between cavitation erosion area and noise characteristics

This section compares the relationship between paint erosion test results and noise measurement results. Figure 9 shows the relationship between the overall noise level and each of the operational conditions, and as in Fig. 6, markers are used to classify the development and form of cavitation in the visualization experiment. The markers are filled in the conditions with surface delamination confirmed by the paint erosion test. The air-borne noise in Fig. 9(a) shows a similar trend with decreasing σ for ϕ/ϕ_d =0.50, 0.70, 1.00, and 1.20, and different trend for σ <0.250. At ϕ/ϕ_d =1.00 and 1.20, there is an increase in noise at higher σ than the operating conditions in both cases with areal exfoliation observed. This range is the transition from sparse exfoliation to areal exfoliation and is considered to capture the collapse of cavitation. Paint erosion tests help to predict in advance the conditions under high risk of erosion. Also, at ϕ/ϕ_d =0.50 and 0.70, the overall value increased rapidly at the 3% drop point of the pump head. The trend was consistent with the results of Dong et al[3], considering the fluid force due to cavitation blockage was converted to acoustic energy. Comparing the suction condition of vortex cavitation in reverse flow at ϕ/ϕ_d =0.30 with other ϕ/ϕ_d conditions, the overall value was decreased. Since the visualization test showed fine bubble clusters and the paint erosion test showed no areal detachment, it is assumed the bubble clusters always weakened the sound propagation without collapsing it. Therefore, predicting cavitation instability phenomena from external noise is difficult with current measurement methods. In addition, the characteristic noise change during the cavitation surge was not observed. The liquid-borne noise in Fig. 10 exhibited similar trends for all ϕ/ϕ_d conditions. Characteristic changes in the noise measurements were not observed for the operating conditions with a high risk of erosion. A previous study[3] showed a positive relationship between the development of cavitation and an increase in noise. The difference in the liquid-borne noise trend indicates the position of the hydrophone. In this study, the hydrophone was installed upstream of the inducer, resulting in the inability to measure localized changes in sound pressure due to cavity collapse. On the other hand, cavitation surge with ϕ/ϕ_d =0.30 indicates significant increase in noise and good response to reverse flow and fluctuations in the internal flow.

FFT analysis was performed on the air-borne noise measurements for each ϕ/ϕ_d condition to confirm the validity for the prediction of erosion risk. Figure 11 shows the results for each ϕ/ϕ_d condition at σ =0.143. The horizontal axis indicates the dimensionless frequency divided by the revolution frequency, and the vertical axis is the sound pressure value [dB] measured at the pressure [Pa] and converted by the equation (4). The BPF of the inducer and impeller and its higher-order components appear in the low frequency range of 25 to 800 Hz. Therefore, discrete specific frequencies due to geometry and flow are affected in the low-frequency range. At high risk of erosion ϕ/ϕ_d =1.00,1.20, the increase was observed in a wide band of high frequencies above 1 kHz. In particular, the increase was significantly larger at 3kHz to 4kHz, and the peak was found to increase around 3.5kHz. These results are similar to the experimental results of Matsumoto et al[14] in their liquid injection method, concluding this phenomenon is the frequency of intermittent release of bubbles from the tail of the cavity. Figure 12 shows the liquid-borne noise at the onset of the cavitation surge; σ =0.051 has a prominent peak below 20 Hz, which is consistent with the frequency

response measured in a previous study[8]. Therefore, it is considered that the air-borne noise was strongly affected by the flow control valve and BPF and could not be captured under the occurrence of cavitation surges.

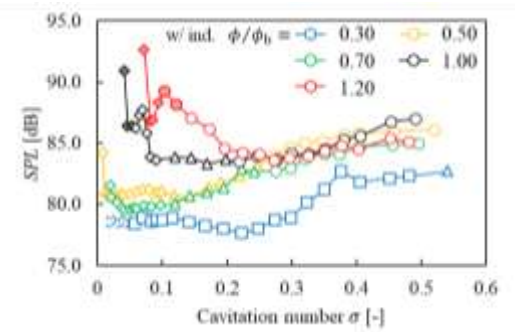

Figure 9. Relationship between cavitation number and air-borne noise

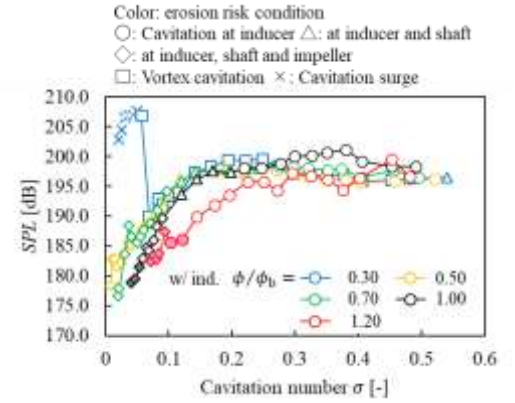

Figure 10. Relationship between cavitation number and liquid-borne noise

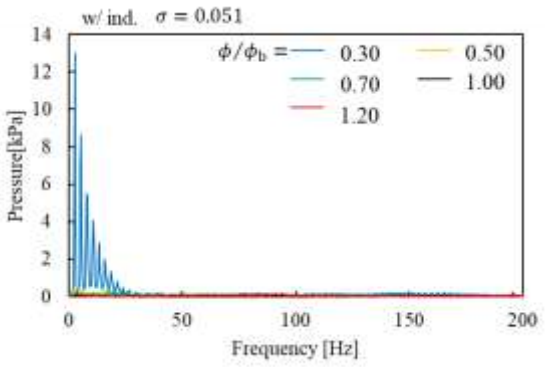

Figure 11. Comparison of air-borne noise spectrum with different flow rate

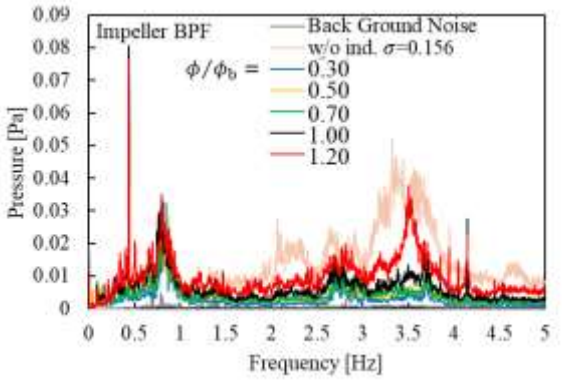

Figure 12. Overall value of high-pass filtered air-borne noise (evaluated range is from 25Hz to 20kHz)

Based on the above results, the measurement in the high-frequency band above 3.0 kHz is considered to be effective for noise evaluation of the risk of erosion. Figure 11 shows the results of applying a high-pass filter above 3.0 kHz in the human audible range of 25 Hz to 20 kHz. It is possible to determine the risk of erosion based on differences in air-borne noise tendency and improve the prediction reliability of erosion risk by using a high-frequency bandwidth.

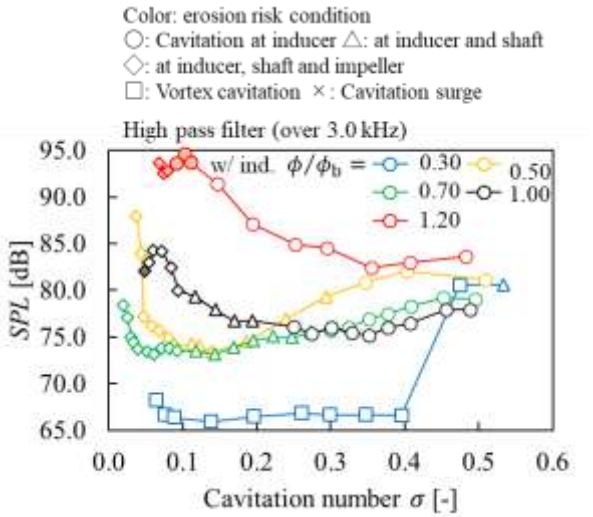

Figure 12. Overall value with 3.0 kHz high pass filter of air-borne noise; 25 Hz to 20 kHz

4.3 Suppression of cavitation erosion by modifying the blades' geometry

Paint erosion experiments showed the area of high erosion risk to be the trailing edge of the inducer blades. Therefore, the geometry of the leading edge of the blade tip was modified to lower the risk of erosion. The effects of applying a borehole or a sweep angle were also investigated. The inducer with the forward sweep angle that had the most significant effect on cavitation instability and noise reduction is shown below. Figure 13 shows the view of the inducer with forward sweep; the leading and trailing edges of the blade tip are swept upstream. In this study, the inlet and outlet angles are the same as the base geometry without the sweep angle. The comparison of the overall values of air-borne noise with and without sweep angle is shown in Fig. 14. Applying the leading edge sweep angle, the noise reduction was confirmed even under the σ condition at ϕ/ϕ_d =1.00, with a high risk of erosion.

The visualization test in Fig. 15 shows the forward sweep is effective in suppressing the development of cavitation generated at the leading edge to the blade tip direction. Furthermore, the paint erosion experiment in Fig. 15 shows the lower risk of erosion, since no areal detachment was observed. These results suggest the cavitation collapse at the inducer blade tip leads to higher risk of erosion with more noise increase. The addition of a forward sweep angle is expected to lower the noise level and decrease the risk of erosion. On the other hand, the sound pressure level did not increase significantly at ϕ/ϕ_d =1.20, although it remained consistently higher than for the other ϕ/ϕ_d conditions. Therefore, employing the forward sweep enables to lower both the noise and the risk of erosion, but further investigation of the blade geometry is required to determine the cause of the noise gain in the high flow region.

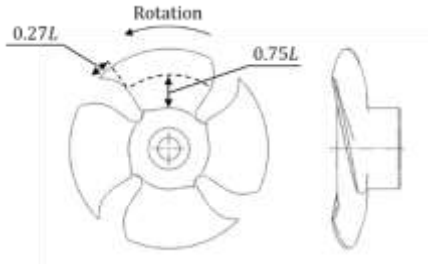

Figure 13. Fan-type inducer with forward sweep

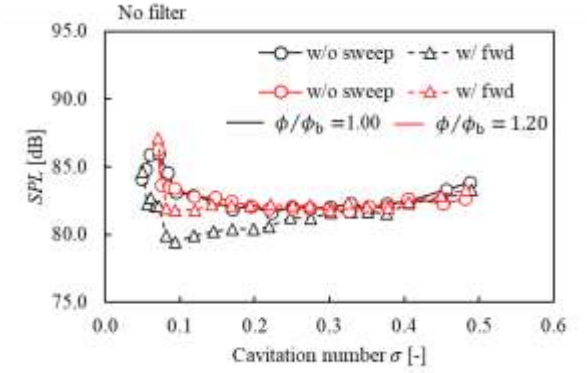

Figure 14. Comparison of air-borne noise with two different inducers

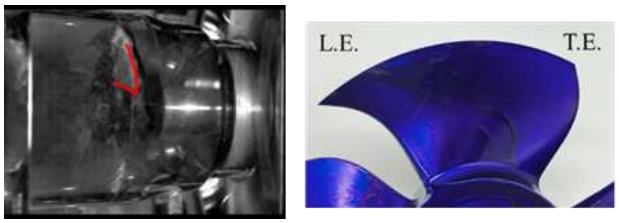

(a) Visualization; σ =0.291 (b) paint erosion; σ= 0.052

Figure 15. Inducer with forward sweep at ϕ/ϕ_d=1.00

5. CONCLUSIONS

- It is possible to predict erosion risk by the tendency of air-borne noise.
- It is also possible to make the prediction accuracy higher using high pass filter over 3.0kHz.
- The cavitation surge can be detected by liquid-borne noise.
- The erosion risk and noise are reduced by adopting the forward sweep geometry.
- The cavitation development near the inducer tip is suppressed by the forward sweep geometry.

6. EQUATIONS

The equations used in this study are shown below.

$$s_t = l_t / t_t \quad (1)$$

$$m_1 = \varphi_{1t} / \tan\beta_{1t} \quad (2)$$

$$\psi = \frac{p_{out} - p_{in}}{\rho u^2} \quad (2)$$

$$\varphi = \frac{Q}{Au^2} \quad (3)$$

$$\sigma = \frac{p_{in} - p_v}{\frac{1}{2}\rho u 2} \quad (4)$$

$$SPL = 10\log_{10}\frac{p^2}{p_0^2} = 20\log_{10}\frac{p}{p_0} \quad (5)$$

$$OA = 10\log_{10}\left(\sum_{i=1}^{n} 10^{\frac{SPL}{10}}\right) \quad (6)$$

7. ACKNOWLEDGMENTS

The authors would like to thank NIKKISO Co., Ltd. For permission to present this paper.

8. REFERENCES

[1] Brennen, C. E., “Hydrodynamics of Pumps”, Cambridge University Press, 1994.

[2] Dong, L., Zhao, Y. and Dai, C., “Detection of Inception Cavitation in Centrifugal Pump by Fluid-Borne Noise Diagnostic”, Hindawi Shock and Vibration, Vol. 2019.

[3] Chudina, M., “Noise as an Indicator of Cavitation in a Centrifugal Pump”, Acoustic Physics, Vol. 49, No. 4, pp. 463-474, 2003.

[4] Černetič, J. and Čudina, M., “Estimating uncertainty of measurements for cavitation detection in a centrifugal pump”, Measurement, Vo. 44, No. 7, pp. 1293-1299, 2011.

[5] Iga, Y., Yokoi, T., Moriya, S., Okajima, R., Nomi, M., ”Noise Measurement of Rotating Cavitation Arising in a Centrifugal Pump (in Japanese)”, Turbomachinery, Vol. 52, No. 6, pp.334-343, 2024.

[6] Fukaya, M., Tamura, Y. and Matsumoto, Y., “Prediction of Cavitation Intensity and Erosion Area in Centrifugal Pump by Using Cavitation Flow Simulation with Bubble Flow Model”, Journal of Fluid Science and Technology, Vol. 5, No. 2, pp. 305-316, 2010.

[7] Miyabe, M. and Maeda, H., “Numerical Prediction of Pump Performance Drop and Erosion Area due to Cavitation in a Double-Suction Centrifugal Feedpump”, Proc. of ASME-JSME-KSME 2011 Joint Fluids Engineering Conference, AJK2011-06023, pp. 121-128, 2011.

[8] Narimatsu, S., Nakayama, S., Konno, S., Ejiri, S. and Miyabe, M., “Analysis of Instability Phenomena Occurring in a Centrifugal Pump with a Low-solidity Fan-type Inducer”, Proc. of the ASME 2024 Fluids Engineering Division Summer Meeting, FEDSM2024-130433, 2024.

[9] Takao, S., Konno, S., Ejiri, S., Miyabe, M., ”Experimental Investigation on the Suppression of Diffuser Rotating Stall in a Centrifugal Pump Using Diffuser Vane Slits (in Japanese)” , Turbomachinery, Vol. 50, No. 2, pp. 101-109, 2020.

[10] Ejiri, S., “Fan Type Inducer for a Centrifugal Pump by Wire Arc Additive Manufacturing and Machining”, International Journal of Fluid Machinery and Systems, Vol. 16, No. 2, pp. 184-191, 2023.

[11] Furukawa, A., Ishizaka, K., “Inducer design and instability phenomena (in Japanese)”, JSME, RC 178, 2002.

[12] Saito, S., “Generation Mechanism and Transition Process of Cavitation Noise”, JSME international journal, Ser. 2, Vol. 32, No. 2, pp. 189-198, 1989.

[13] Turbomachinery Society of Japan, ”Guideline for Prediction and Evaluation of Cavitation Erosion in Pumps (in Japanese)”, TSJ G 011: 2011, 2016

[14] Matsumoto, M., Inoue, Y., Kobashi, Y., Matsumura, E., Senda, J., ”Effect of Cavitation inside Injection Nozzle on Spray Characteristics for Direct Injection”, Transactions of the Japan Society of Mechanical Engineers, Part B, Vol. 79, No. 806, 2013.